Journal of Power Sources 189 (2009) 1184–1189

Contents lists available at ScienceDirect

Journal of Power Sources

journal homepage: www.elsevier.com/locate/jpowsour

Performance of Li-ion secondary batteries in low power, hybrid power supplies

Shruti Prakash[a], William E. Mustain[b], Paul A. Kohl[a,*]

[a] School of Chemical and Biomolecular Engineering, Georgia Institute of Technology, Atlanta, GA 30332-0100, United States
[b] Department of Chemical, Materials and Biomolecular Engineering, University of Connecticut, Storrs, CT 06269, United States

ARTICLE INFO

Article history:
Received 3 November 2008
Received in revised form 24 December 2008
Accepted 24 December 2008
Available online 17 January 2009

Keywords:
Lithium ion battery
Hybrid power source

ABSTRACT

Small, portable electronic devices need power supplies that have long life, high energy efficiency, high energy density, and can deliver short power bursts. Hybrid power sources that combine a high energy density fuel cell, or an energy scavenging device, with a high power secondary battery are of interest in sensors and wireless devices. However, fuel cells with low self-discharge have low power density and have a poor response to transient loads. A low capacity secondary lithium ion cell can provide short burst power needed in a hybrid fuel cell–battery power supply. This paper describes the polarization, cycling, and self-discharge of commercial lithium ion batteries as they would be used in the small, hybrid power source. The performance of 10 Li-ion variations, including organic electrolytes with $Li_xV_2O_5$ and $Li_xMn_2O_4$ cathodes and LiPON electrolyte with a $LiCoO_2$ cathode was evaluated. Electrochemical characterization shows that the vanadium oxide cathode cells perform better than their manganese oxide counterparts in every category. The vanadium oxide cells also show better cycling performance under shallow discharge conditions than LiPON cells at a given current. However, the LiPON cells show significantly lower energy loss due to polarization and self-discharge losses than the vanadium and manganese cells with organic electrolytes.

1. Introduction

The recent growth in the deployment of ultra low power (<100 μW average power) wireless devices for sensing and communication has led to the search for a suitable high energy density power supply. Ultra low power direct methanol fuel cells (DMFC) have the promise to provide power with the highest possible energy density. However, micro DMFCs suffer from the same drawbacks as traditional DMFCs and PEM fuel cells for portable power applications, namely their inability to adjust to transient loads with acceptable efficiency. Therefore, many fuel cell systems must rely on a hybrid architecture, such as the one shown in Fig. 1, where a secondary energy storage device provides the high current response to the transient load and the fuel cell provides a steady-state current that operates the circuit controls and recharges the energy storage device.

Secondary lithium ion (Li-ion) batteries are the preferred energy storage device for many high power portable applications including cellular phones, laptop computers, and hybrid electric vehicles. Li-ion cells are the best option for the fuel cell–battery hybrid power source due to their high energy density, good cyclability, and high energy efficiency compared to previous battery technologies, including nickel–cadmium, nickel-metal hydride, and zinc–air. However, Li-ion batteries also suffer from energy losses during cycling and self-discharge, both of which are a function of the state-of-charge. In this hybrid fuel cell–battery application, there are losses due to self-discharge and the discharge polarization. The purpose of this study was to evaluate the trade-offs between battery type, state-of-charge, and battery capacity in order to find the most energy efficient operating condition.

The kinetics of self-discharge will vary greatly depending on the battery chemistry, electrode composition and electrolyte formulation. Most Li-ion manufacturers use similar non-aqueous electrolytes, which consist of $LiPF_6$ solvated in linear and cyclic carbonates such as dimethyl carbonate and ethylene carbonate, respectively [1,2]. The most widely used cathode since the 1990s is Li_xCoO_2 [3–7]. However several other cathodes are used including $Li_xMn_2O_4$ [8–10], Li_xNiO_2 [11,12], and $Li_xV_2O_5$ [4–6,10,13]. A solid-state electrolyte, lithium phosphorus oxynitride electrolyte (LiPON) has been developed and shown to have high power, low self-discharge, and long life [14]. The glassy behavior of the electrolyte provides stabile contact with the electrodes, which provides the low self-discharge. The presence of nitrogen atoms in amorphous matrix of lithium phosphate is responsible for the increased stability of the battery [15].

In a previous study by Johnson and White [16], it was shown that the self-discharge of a commercial Sony 18 650 battery, which has a $LiCoO_2$ cathode, operating at approximately 4.0 V is 11 μA cm^{-2},

* Corresponding author.
E-mail address: Paul.Kohl@chbe.gatech.edu (P.A. Kohl).

0378-7753/$ – see front matter © 2009 Elsevier B.V. All rights reserved.
doi:10.1016/j.jpowsour.2008.12.146

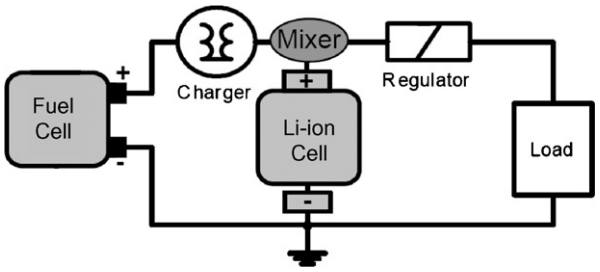

Fig. 1. Hybrid fuel cell-lithium ion power supply.

which the authors noted as "negligible". This self-discharge current can be considered negligible when the average discharge rate is high, such as a laptop with a 1.2 Ah battery operating at a C/4 discharge. However, in small sensor applications, the steady-state current may be only 100–500 μA and the battery may only operate at C/4 discharge rate less than 0.1% of the devices' life.

Small Li-ion batteries can be used in hybrid power supply applications, however, they must meet the peak power needs of the system, which can be from 1 mA to 50 mA, without wasting excessive energy through self-discharge. Very small sensors which require only a steady-state trickle charge, for example 10 μW, are very vulnerable to self-discharge problems. Over-sizing the battery would waste fuel cell energy in self-discharge while under-sizing the battery would result in system failure because the peak power needs would not be met.

Thus, the self-discharge current of Li-ion batteries is an important parameter in designing ultra low power, hybrid power sources. One design parameter of importance in the battery is the active area. It should be as low as possible in order to minimize the self-discharge but be large enough to supply the peak power. Many sensors have low average power with short bursts of activity. For example, in many cases the peak current, i_1 (Fig. 2) can be 1000 times greater than the steady-state sleep current, i_2, unlike larger electronic systems where the current ratio may only be 5:1. Also, the duty cycle is low, i.e. $t_2 \gg t_1$. It is clear that the use of Li-ion cells in ultra low power applications is altogether different than their use in larger electronic systems. The depth-of-discharge during the brief, high current bursts is typically less than 1% of the stored charge. The battery is recharged between events so that the battery spends most of its life a zero net current, except for the recharge current which must be supplied to compensate for self-discharge. Therefore, cell selection requires a balance between the polarization and self-discharge loss. The goal here is to find the Li-ion technology which can provide brief, high current bursts with as low as possible self-discharge.

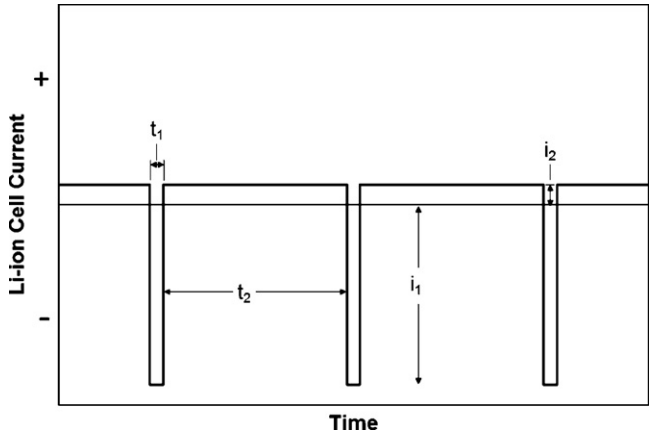

Fig. 2. Current pulse profile for secondary Li-ion cell in a hybrid power supply.

In this investigation, we quantify the self-discharge and polarization losses of ten commercially available lithium ion cells as a function of cell potential. Since energy density, rechargeability and discharge rate are mainly dependent on the cathode material, we investigated cells with similar anodes and electrolytes. $Li_xV_2O_5$ and $Li_xMn_2O_4$, cathodes were investigated. In addition, one LiPON electrolyte cell with a $LiCoO_2$ cathode was also investigated.

2. Experimental

Ten low capacity Li-ion coin-type cells were used in this investigation. Each study used a minimum of three cells. The response across each set of cells was consistent. In order to maintain similarity between the electrode and electrolyte a single manufacturer, Panasonic, was used for nine of the cells. In order to look at the effect of the electrolyte, a thin film LiPON electrolyte cell was purchased from Front Edge Technology, Inc. The physical parameters of the commercial cells are presented in Table 1.

All electrochemical measurements were made with an Arbin battery test system. For each experiment, new cells were used in order to eliminate the effect of capacity and performance fading caused by cycling.

In order to confirm the cell capacity, cycling tests were done between 2.5 and 4.2 V in the galvanostatic mode with charge and discharge currents of 100 μA. Following cycling, the cells were dissected and the normalizing area for all other experiments was taken as the cathode geometric area. Cell polarization and charge-loss experiments were conducted by charging the cells at 1/100 C to the desired voltage. Four cell voltages were of interest in this study: 3.5, 3.75, 4.0 and 4.2 V. For the polarization experiments, the cells were immediately discharged (immediately following the charge cycle) at 1/10, 1/5, 1/2, 1, or 2 C relative to their rated capacity for 1 s. The cells were recharged at 1/100 C until the original voltage was achieved and the charge/discharge cycle was repeated 50 times with each cell. The discharge potential was taken as the peak (minimum) value measured using the Arbin system. The value reported here was calculated by taking the mean of the final five discharge values for each of the tested cells.

The self-discharge, or ability to recover the charge stored within the battery (i.e. coulombic efficiency) is an important parameter for the secondary batteries considered here. The self-discharge rate of the battery during hybrid power source operation was investigated by cycling at four discharge rates. The cell was first charged to one of four voltages of interest: 3.5, 3.75, 4.0 or 4.2 V. The cell was then discharged for 100 s at constant current. The cell was then recharged at the same current as that used in the discharge until the original cell voltage was reached. The recharge time was greater than 100 s and the time varied based on cell size, chemistry and charge/discharge current. For smaller cells, with capacities lower than 20 mAh, the cells were discharged and recharged at 2, 6, 8 and 10 μA. For larger cells, the current was increased by a factor of either 2 or 5.

3. Results and discussion

The capacity of the commercial Li-ion cells was tested in order to determine the portion of the rated capacity available between 2.5 and 4.2 V. The results for ML621, VL621 and NX0201 cells are shown in Fig. 3. For the ML621, the available capacity is nearly a linear function of the charge voltage. This was repeated for 20 cycles for three different cells. This is somewhat different than results previously reported for laboratory prepared Li-ion cells with a $Li_xMn_2O_4$ cathode [17,18]. However, this phenomenon has been observed previously in the literature with solid electrolytes [19] and carbon composite electrodes [20].

Table 1
Properties of tested Li-ion cells.

Cell	Cathode	Electrolyte	Manufacturer	Nominal capacity (mAh)	Diameter (mm)	Height (mm)	Active diameter (mm)	Active area (cm^2)
ML414	MnO_2	Organic	Panasonic	1.2	4.8	1.4	2.9	0.07
ML621	MnO_2	Organic	Panasonic	5.0	63	21	42	0.14
ML1220	MnO_2	Organic	Panasonic	17.0	12.5	2 0	10	0.71
ML2020	MnO_2	Organic	Panasonic	45.0	20.0	2 0	16	1.9
VL621	V_2O_5	Organic	Panasonic	15	63	21	0 5	0.17
VL1220	V_2O_5	Organic	Panasonic	7.0	12.5	2 0	10	0.74
VL2020	V_2O_5	Organic	Panasonic	20.0	20.0	2 0	16	2.1
VL2320	V_2O_5	Organic	Panasonic	30.0	23.0	2 0	2 0	3.1
VL2330	V_2O_5	Organic	Panasonic	50.0	23.0	3 0	2 0	3.1
NX0201	CoO_2	LiPON	Front Edge Technology	0.4	N/A	0.2	N/A	3.5

The vanadium oxide cell, VL621, showed two regions during cycling, which is consistent with reported behavior of polycrystalline V_2O_5 cathode Li-ion cells [21,22]. Between 2.5 and 3 V, there is nearly zero stored charge. Between 3.0 and 3.2 V, 110% of the rated capacity is available. This provides a very stable, and desirable performance range. That is, one can use the full capacity of the battery at nearly constant voltage. Overcharging of the V_2O_5 cells resulted in a steep rise in the voltage with minimal gains in the stored charge.

Finally, the NX0201 cell with the LiPON electrolyte and Li_xCoO_2 cathode showed minimal charge storage capability below 3.8 V. At voltages higher than 3.8 V, a steady, linear voltage increase was observed throughout the duration of the charge cycle.

Li-ion cells are operated at relatively high voltage corresponding to a high free energy change between the reactant and product states. There are several contributors to self-discharge in electrochemical systems including faradaic processes due to decomposition of either the electrode or the electrolyte. A portion of the self-discharge occurs during recharge, where the cell voltage is raised higher than the open circuit voltage.

The coulombic efficiency (fraction of the stored charge which can be recovered), or self-discharge, is especially important in hybrid, portable power sources because it compromises the energy density of the primary energy source, the fuel cell, by adding an additional load. In the hybrid sources considered here, the battery spends most of its time at open circuit or being recharged at a low C-rate. Typically, the self-discharge rate is used to evaluate the shelf-life of an electrochemical cell and is measured by fully charging the cell, allowing it to sit at open circuit for a period of time and then discharging the cell at low current. The columbic difference between the charge and discharge steps is then divided by the open circuit time. The self-discharge is given as the average current accounting for the lost charge. In the case of a hybrid power supply, open circuit shelf-life is not an issue. Rather, the charge lost during recharge at low C-rate following a shallow discharge cycle more closely captures the operating mode of the hybrid power source.

In this work, the self-discharge was evaluated as function of cell potential for an operation mode which closely matches the performance of a battery in the hybrid power source. The batteries were charged to the operating voltage of interest: 3.5, 3.75, 4.0, and 4.2 V. The cells were then discharged at low current for 100 s corresponding to a very low depth-of-discharge, below 0.1%, which is typical of the discharge of the battery during operation in the hybrid power source. The cells were recharged at the same current to the original operating voltage. The recharge time was greater than 100 s in each case. The time in excess 100 s accounts for the excess charge which has been supplied due to self-discharge. The loss in charge is represented as a self-discharge current, i_{SD}, by averaging the charge over the time for the whole cycle, Eq. (1).

$$i_{SD} = \frac{i_c(t_c - t_d)}{t_c + t_d} \quad (1)$$

where i_c is the charging current, t_c is the recharge time, and t_d the discharge time, 100 s. The self-discharge were evaluated for all 10 Li-ion cells listed in Table 1. A representative summary of those results, providing a full picture of the performance, is provided. At least three duplication cells were tested in each case. The data points shown are the result of the average of the final five cycles of each cell and the error in all measurements was taken as 3 times the standard deviation.

The self-discharge for VL621 lithium ion cells was measured at 4.2 V with charge/discharge currents of 10, 8, 6 and 2 μA and is shown in Fig. 4. The loss due to self-discharge increased with the charge current. As expected, the self-discharge increased with charging current when the electrode overpotentials were the highest.

Identical experiments were performed with the NX0201 cells at 4.2 V with charge/discharge currents of 1.0, 0.8, 0.6 and 0.2 μA,

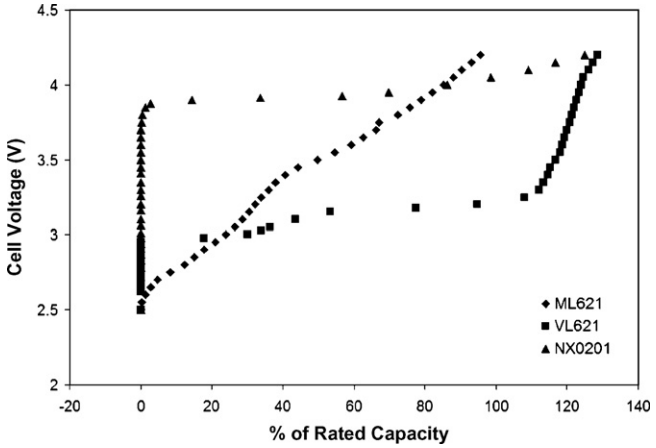

Fig. 3. Cell voltage vs. rated capacity for ML621, VL621 and NX0201 cells.

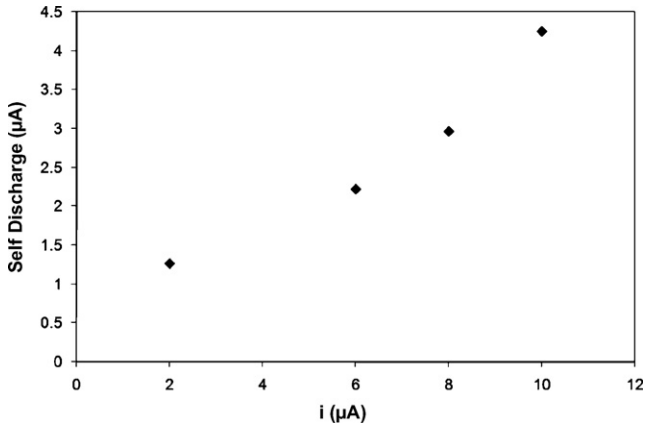

Fig. 4. Self-discharge current vs. charge/discharge current for VL621 Li-ion cells.

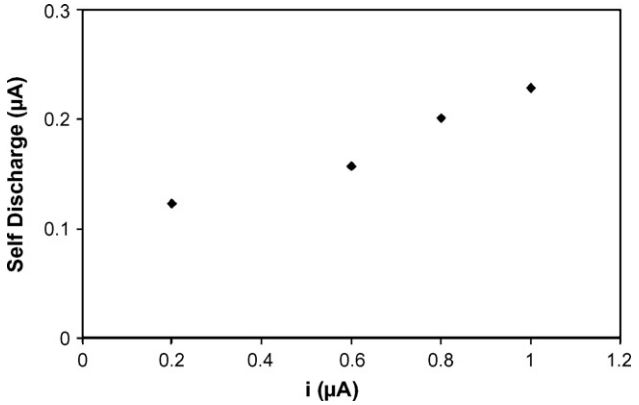

Fig. 5. Self-discharge current vs. charge/discharge current for Front Edge NX0201 thin film Li-ion cells charged to 4.2 V.

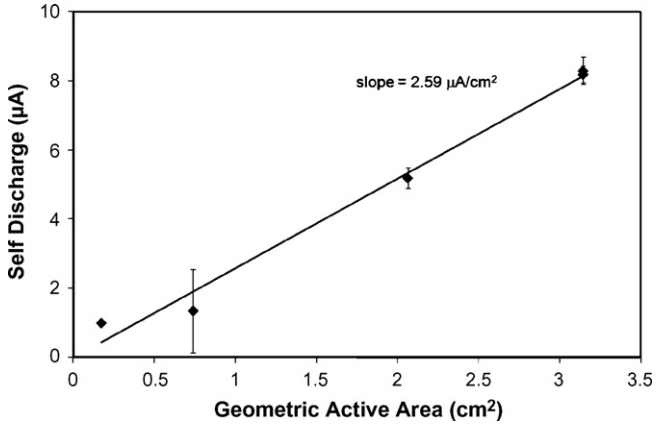

Fig. 8. Self-discharge of VL series lithium ion button cells at 3.75 V.

as shown in Fig. 5. The magnitude of the self-discharge was less than the VL621. The self-discharge current for the NX0201 was much less than with self-discharge for the vanadium oxide cell, even though its electrochemically active area is significantly larger. This is consistent with literature reports that LiPON electrolyte cells show significantly lower self-discharge than their counterparts with organic electrolytes [19,23–25].

The self-discharge for all cells was also investigated as a function of the operating voltage. The self-discharge of VL1220 and ML414 cells as a function of voltage are shown in Figs. 6 and 7, respectively. Overall, the self-discharge of the lithium ion cells increased with cell voltage due to the higher overpotentials at the electrode surfaces during recharge. This was also the case for the LiPON electrolyte thin film cell. The self-discharge is function of the state-of-charge for the vanadium oxide cells and rapidly increases at higher a higher state-of-charge (higher voltage). For example, the self-discharge increases more than 10 times when the voltage increased from 3.5 to 4.0 V. For the manganese cells, the effect is less pronounced, showing only a 2.5 fold increase over the same voltage range. This may be due to similar states of charge for the manganese cells at 3.5 and 4.0 V, shown in Fig. 3. The geometric area of the cells was measured by disassembling three of each type of battery and measuring the area of the cathode pellet. This was done for the vanadium oxide and manganese oxide cathode cells. The self-discharge density (self-discharge per unit area) can be determined for the ML and VL series cells, as shown in Figs. 8 and 9, respectively, at 3.75 V. The self-discharge for the VL series and ML series cells compares favorably with previously reported $LiCoO_2$ cathode cells measured at open circuit at similar voltages, 11 $\mu A\,cm^{-2}$ [16]. Improvements in the Li-ion cathode have led to a reduction in the self-discharge. Also, the results for the self-discharge of VL2320 and VL2330 cells shown in Fig. 8 verify that the self-discharge is a function of the electrode surface area exposed to the electrolyte and not the cell capacity.

The vanadium cells generally have lower self-discharge than their manganese counterparts, even though the cells were constantly operated in the overcharge region. The overcharge caused the self-discharge of the VL cells to significantly increase at high voltage where it surpassed that of the ML cells above 4.0 V. Both

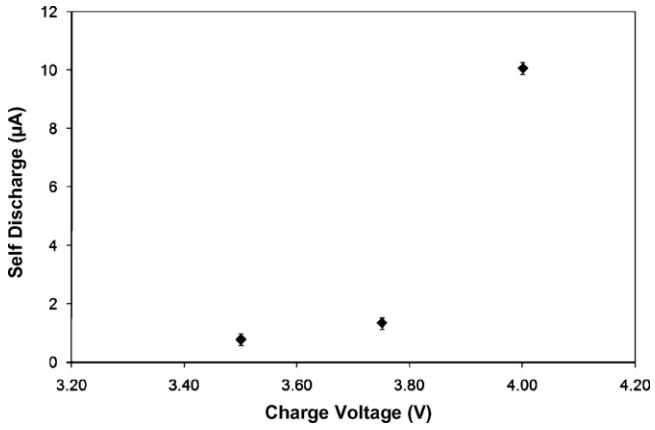

Fig. 6. Self-discharge current vs. charge voltage for VL1220 cells.

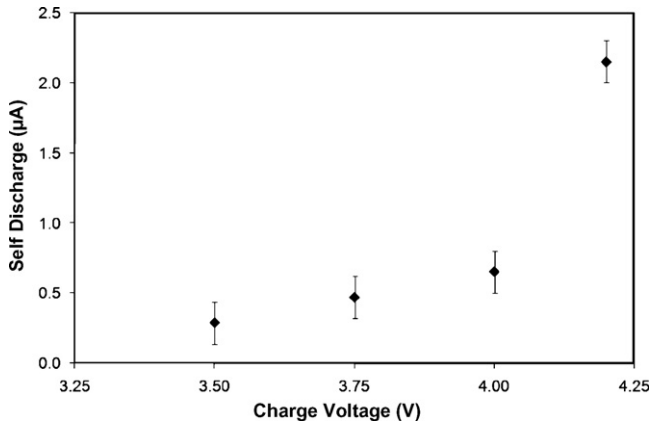

Fig. 7. Self-discharge current vs. charge voltage for ML414 cells.

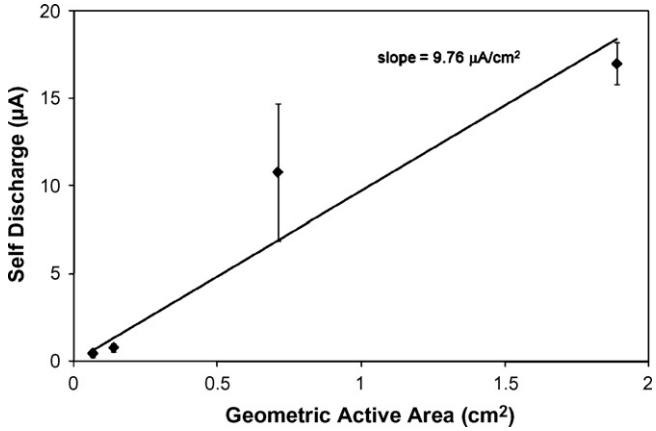

Fig. 9. Self-discharge of ML series lithium ion button cells at 3.75 V.

Table 2
Discharge efficiency as a function of discharge rate and charge potential for ML414 cells.

Voltage	Discharge rate				
	2 C	1 C	1/2 C	1/5 C	1/10 C
4.20	0.26	0.59	0.77	0.91	0.94
4.00	0.60	0.78	0.88	0.96	0.97
3.75	0.45	0.68	0.82	0.93	0.95
3.50	0.43	0.67	0.81	0.93	0.95

Cell	Cathode	Electrolyte	Manufacturer	Nominal capacity (mAh)	Diameter (mm)	Height (mm)	Active diameter [mm]	Active area (cm^2)
ML414	MnO_2	Organic	Panasonic	1.2	4.8	1.4	2.9	0.07
ML621	MnO_2	Organic	Panasonic	5 0	6.8	2 1	42	0.14
ML1220	MnO_2	Organic	Panasonic	17.0	12.5	2 0	1 0	0.71
ML2020	MnO_2	Organic	Panasonic	45.0	20.0	2 U	1 6	1.9
VLB21	V_2O_5	Organic	Panasonic	1 5	5 8	2 1	0.5	0.17
VL1220	V_2O_5	Organic	Panasonic	^{7} 0	125	2 0	1 0	0.74
VL2020	V_2O_5	Organic	Panasonic	20.0	20.0	2 0	1 6	2.1
VL2320	V_2O_5	Organic	Panasonic	30.0	23.0	2 0	2.0	3.1
VL2330	V_2O_5	Organic	Panasonic	50.0	23.0	3 0	2 0	3.1
NX0201	CoO_2	LiPON	Front Edge Technology	0.4	N/A	0.2	N/A	3.5

the ML and VL series cells have inferior performance to the NX0201 thin film LiPON cell.

Although the self-discharge can play an important role in energy efficiency, the self-discharge rates were generally acceptable for hybrid power supplies. The main energy loss encountered in the hybrid power supply is the energy loss due to electrode polarization. When a cell is discharged, the potential difference between the two electrodes is less than during charging due to electrode polarization. At zero current, the cell remains at open circuit voltage. As the cell is discharged, the cell voltage drops, due to activation and concentration overpotential. The potential difference between charging and discharging increases with current density and thus lowers the energy efficiency. The discharge efficiency, ε, can be defined as the average discharge voltage, V_d, divided by the average charging voltage, V_c, as shown in Eq. (2).

$$\varepsilon = \frac{V_d}{V_c} \tag{2}$$

The discharge efficiency is not a significant concern when plug-power is used to recharge the lithium ion cell because of the virtually unlimited supply of current. In the case of a fuel cell powered hybrid, the energy loss due to discharge efficiency can be a significant energy drain.

Cell polarization measurements were performed on all cells at 2, 1, 1/2, 1/5, and 1/10 C rates. The results for the ML414 cells are presented in Table 2. The cells show two clear trends. First, the discharge efficiency improves as the C-rate is decreased. This was true for all the cells tested at 4.2, 4.0, 3.75 and 3.5 V. Second, the peak efficiency at all rates was observed at 4.0 V. This is likely a balance of two effects. First, the activation overpotential increases as the discharge rate increases. Second, as the discharge rate is increased, the number of lithium ions available for deintercalation at the Li-ion anode is reduced, leading to a depletion overpotential at the electrode surface due to mass transport. Thus, the higher state-of-charge and lower discharge C-rate favor improved energy efficiency.

Table 3
Discharge efficiency as a function of discharge rate and charge potential for VL1220 cells.

Voltage	Discharge rate				
	2 C	1 C	1/2 C	1/5 C	1/10 C
4.20	0.69	0.79	0.86	0.92	0.94
4.00	0.75	0.85	0.91	0.97	0.98
3.75	0.76	0.85	0.91	0.97	0.98
3.50	0.78	0.86	0.92	0.97	0.98

Identical experiments were conducted with VL1220 cells and are given as Table 3. As in the previous case, the cell polarization decreases at lower C-rate. However, for the vanadium oxide cells, the highest efficiencies were observed at the lowest tested cell voltage, 3.5 V, at all rates, although there was only a modest increase over the performance at 4.0 V. In the most extreme case, 4.2 V operating voltage and 2 C discharge, the efficiency for the VL series cell is 165% greater than the ML series. At modest conditions, 3.5 V and C/10, only a 3% improvement was realized.

Polarization experiments were also performed with the NX0201 thin film LiPON cell, which are summarized in Table 4. As with other cells, the discharge efficiency increased with decreasing C-rate. However, in this case the efficiency steadily improved from 3.5 to 4.2 V. This is clearly due to the LiPON operating window and higher state-of-charge at high voltage, as shown in Fig. 3. The LiPON cell had nearly zero stored charge below 3.8 V.

Table 4
Discharge efficiency as a function of discharge rate and charge potential for NX0201 cells.

Voltage	Discharge rate				
	2 C	1 C	1/2 C	1/5 C	1/10 C
4.20	0.982	0.991	0.995	0.998	0.999
4.00	0.981	0.991	0.995	0.998	0.999
3.75	0.843	0.922	0.963	0.989	0.995
3.50	0.737	0.864	0.922	–	0.981

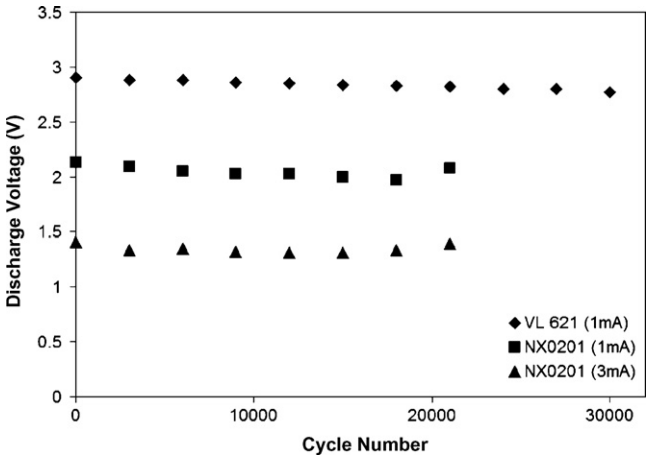

Fig. 10. Discharge voltage as a function of cycle number for shallow discharge experiments with vanadium oxide cathode VL621 and LiPON electrolyte NX0201 cells.

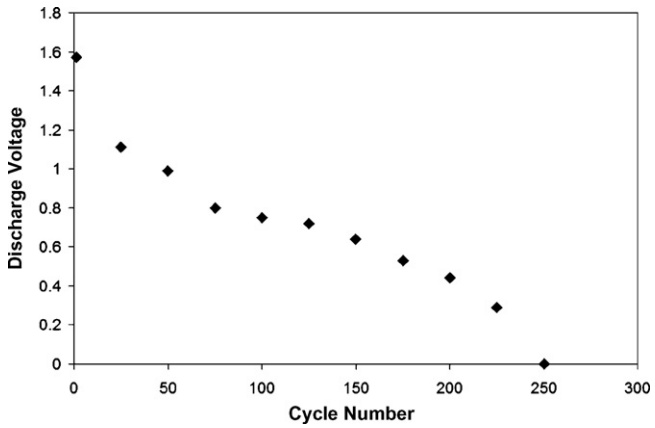

Fig. 11. Discharge voltage as a function of cycle number for VL621 cells discharged at 3 mA.

The cell polarization experiments are useful in determining the performance of the cells during operation, however, other factors contribute to the battery's performance during the hybrid cell's lifetime. Capacity-fade of batteries can occur during cycling. However, in this investigation, the depth-of-discharge for each cycle is low, which reduces the risk of capacity face. Second, a 2 C discharge rate for the NX0201 cell corresponds to less than C/10 for the ML621 and 0.5 C for the VL 621, both of which have a much higher capacity at the same cell volume and lower surface area.

In order to compare the performance of the thin film LiPON cell with the higher capacity VL cell of comparable volume, the discharge experiments were performed at 1 and 3 mA with NX0201 and VL621 cells charged to 3.5 V. Fig. 10 shows the cell voltage during discharge for the NX0201 (at 1 and 3 mA) and the VL621 cell (at 1 mA) as a function of cycle number. All three cells show stable performance with cycle number during these shallow discharge experiments. However, the discharge voltage at 1 mA was significantly higher than for the VL 621 cell than the NX0201. The volumes of the two cells were approximately the same, however the capacity of the VL 621 was higher than the NX0201. A 1 mA discharge represents only a 0.67 C discharge for the VL621, whereas the same current is a 2.5 C discharge for the NX0201. However, the NX0201 has a larger electrode area than the VL621 and the NX0201 has limited capacity at low discharge voltages, whereas the VL series cell is almost fully charged (Fig. 3).

The voltage efficiency of all cells decreased slowly with cycling. The VL621 cells showed a 4.5% decrease in the discharge voltage after 30,000 cycles. On the other hand, the LiPON cells showed a decrease of 7.5% and 5.7% for the 1 and 3 mA experiments, respectively. The NX0201 cell performance became erratic at 21,000 cycles, sometimes showing negative discharge potentials or an inability to reach the desired discharge rate and the experiments were terminated. The high discharge rate for the NX0201 (3 mA corresponds to 7.5 C) is likely a contributing factor in overstressing the cell.

Fig. 11 shows the low depth-of-discharge cycling performance for the VL621 cell with a 3 mA discharge pulse. The cell shows a rapid decrease in performance with cycle number and no useful work is obtained after 250 cycles. Therefore, for the vanadium oxide cells to be competitive, one needs to oversize the cell such that the discharge is no greater than 1 C, while the thin film LiPON cells are clearly superior at high C-rates, although efficiency is sacrificed.

4. Conclusions

Several commercial secondary Li-ion cells have been investigated for use in low power hybrid power supplies. The self-discharge of the LiPON electrolyte cells was found to be more than an order of magnitude superior to the manganese and vanadium oxide cathode cells with organic electrolytes despite their larger electrode area. However, the manganese oxide and vanadium oxide cell showed a superior self-discharge behavior to previously reported commercial cells with a $LiCoO_2$ cathode and similar electrolyte. Their self-discharge values were 9.76 and 2.59 $\mu A\,cm^{-2}$.

The cells were also tested for their polarization performance and lifetime stability with low depth-of-discharge pulses. The LiPON NX0201 cell showed the best polarization performance to any other cell, though it should be noted that the vanadium oxide cells showed a much higher efficiency, as high as 165%, than manganese oxide cells under identical operating conditions. Finally, both the vanadium oxide cathode and LiPON electrolyte cells showed excellent cycling performance at low depth-of-discharge, <0.01% depth-of-discharge. The performance of the LiPON cells was stable for 21,000 cycles at 7.5 C, while the vanadium oxide cells were stable at 2/3 C for over 30,000 cycles. However, at 2 C the cycling performance of the vanadium oxide cells was poor, yielding usable power for only 250 cycles with efficiencies always less than 45%.

Acknowledgements

The authors would like to thank the Test Resource Management Center (TRMC) Test and Evaluation/Science and Technology (T&E/S&T) Program for their support. This work is funded by the T&E/S&T Program through the Naval Undersea Warfare Center, Newport, RI, contract number N66604-06-C-2330.

References

[1] G.E. Blomgren, J. Power Sources 82 (1999) 112.
[2] H. Kim, H.J. Sohn, T. Kang, J. Electrochem. Soc. 146 (1999) 4401.
[3] K. Mizushima, P.C. Jones, P.J. Wiseman, J.B. Goodenough, Mater. Res. Bull. 15 (1980) 783.
[4] J.B. Bates, N.J. Dudney, D.C. Lubben, G.R. Gruzalski, B.S. Kwak, X. Yu, R.A. Zuhr, J. Power Sources 54 (1995) 58.
[5] J.G. Zhang, J.M. McGraw, J. Turner, D. Ginley, J. Electrochem. Soc. 144 (1997) 1630.
[6] Y.J. Park, K.S. Ryu, K.M. Kim, N.G. Park, M.G. Kang, S.H. Chang, Solid State Ionics 154 (2002) 229.
[7] O. Kazunori, M. Yokokawa, 10th International Seminar of Primary and Secondary Battery Technology Applications, 1–4 March 1993, Deerfield Beach, FL, USA, Florida Educational Seminars, Boca Raton, FL, 1993.
[8] F.K. Shokoohi, J.M. Tarascon, B.J. Wilkens, Appl. Phys. Lett. 59 (1991) 1260.
[9] F.K. Shokoohi, J.M. Tarascon, B.J. Wilkens, D. Guyomard, C.C. Chang, J. Electrochem. Soc. 139 (1992) 1845.
[10] N. Kumagai, H. Kitamoto, M. Baba, S. Durand-Vidal, D. Devilliers, H. Groult, J. Appl. Electrochem. 28 (1998) 41.
[11] J.R. Dahn, U. Von Sacken, M.R. Jokow, H. Al-Janaby, J. Electrochem. Soc. 137 (1991) 2207.
[12] A. Hirano, R. Kanno, Y. Kawamoto, Y. Takeda, K. Yamamura, M. Takano, K. Ohyama, M. Obhashi, Y. Yamaguchi, Solid State Ionics 78 (1995) 123.
[13] C. Delmas, S. Brethes, M. Menetrier, J. Power Sources 34 (1991) 113.
[14] J.B. Bates, N.J. Dudney, B. Neudecker, A. Ueda, C.D. Evans, Solid State Ionics 135 (2000) 33.
[15] X. Yu, J.B. Bates, G.E. Jellison Jr., F.X. Hart, J. Electrochem. Soc. 144 (2) (1997) 524.
[16] B.A. Johnson, R.E. White, J. Power Sources 70 (1998) 48.
[17] A. Blyr, A. Du Pasquier, g. Amatucci, T.M. Tarascon, Ionics 3 (1997) 321.
[18] A. Blyr, C. Sigala, G. Amatucci, D. guyomard, Y. Chabre, J.M. Tarascon, J. Electrochem. Soc. 145 (1998) 194.
[19] N.J. Dudney, J. Power Sources 89 (2000) 176.
[20] J. Lee, J.M. Lee, S. Yoon, S.O. Kim, J.S. Sohn, K.I. Rhee, H.J. Sohn, J. Power Sources 183 (2008) 325.
[21] K. West, B. Zachau-Christiansen, T. Jacobsen, J. Power Sources 43–44 (1993) 127.
[22] E.J. Jeon, Y.W. Shin, S.C. Nam, W.I. Cho, Y.S. Yoon, J. Electrochem. Soc. 148 (2001) A318.
[23] J.M. Tarascon, C. Schmutz, A.S. Gozdz, P.C. Warren, F. Shokoohi, MRS Symp. Proc. 369 (1994) 595.
[24] T. Gozdz, C. Schmutz, T.M. Tarascon, US Patent 5,296,318 (1996).
[25] J.M. Tarascon, A.S. Gazdz, C. Schmutz, f. Shokoohi, P.C. Warren, Solid State Ionics 86 (1996) 49.